

An Ultra-deeply anchored GPS station in Tsukuba, Japan – preliminary report –

**Hiroshi MUNEKANE, Yuki KUROISHI, Yuki HATANAKA , Kazuhiro TAKASHIMA,
Masayoshi ISHIMOTO and Mikio TOBITA**

Abstract

We installed a GPS station in the premises of the Geographical Survey Institute in Tsukuba. The station is directly attached to the inner tube of a subsidence observation well, anchored at a depth of 190 m, so that it is less affected by seasonal elastic deformations of shallow soils due to groundwater extraction for irrigation. We evaluated the quality of the station by comparing the GPS-derived vertical displacements with those from two independent measurements; subsidence-meter and leveling. For comparison, we prepared two sets of GPS solutions with different analysis strategies; 1) short-distance strategy: where we analyze GPS carrier-phases on L1 and L2 frequencies independently to estimate baseline components only, and 2) long-distance strategy: where we analyze ionosphere-free combinations of GPS carrier-phases on L1 and L2 frequencies to estimate tropospheric delays as well as baseline components. We found that while the GPS-derived vertical displacements in the short-distance strategy generally agree with those from the independent measurements, those in the long-distance strategy systematically disagree. We also noticed that the GPS-derived vertical displacements in both strategies have noticeable common errors in winter. We found that the disagreement of the displacements in the short-distance strategy are errors caused by the multipath from the surface of the roof of the room housing the subsidence observation well, and the latter errors are caused by water droplets formed inside the radome because of water condensation in the room's air in winter. These errors should be mitigated before this station can be utilized as a reliable reference station.

1. Introduction

Space geodetic stations in the premises of the Geographical Survey Institute (GSI) in Tsukuba have played an important role as reference stations in realizing a global reference frame as one of the oldest stations in Asia. The GPS station *TSKB*, in operation since 1993, and the VLBI station *TSUKUBA32*, in service since 1998, are collocated with each other, and are used in the realization of the International Terrestrial Reference Frames (ITRF) (e.g. Altamimi et al., 2007). Moreover, GPS station *92110*, in operation since 1994, has been used as a reference site in the routine analysis of the GEONET (Hatanaka et al., 2005).

As a reference station, it is desirable for the station to be stable with little local deformation. Unfortunately, it is known that anomalous seasonal vertical deformations are observed at *TSKB* and *92110*. Tobita et al. (2004) and Munekane et al. (2004) investigated these annual vertical deformations and

concluded that the deformations are caused by elastic responses of aquifers associated with seasonal extraction of groundwater for irrigating the surrounding rice fields.

GSI installed a device called a “subsidence-meter” in the premises of GSI that allows us to monitor the seasonal vertical deformations. The subsidence-meter is composed of a well of 190 m in depth with dual tubes and an instrument measuring the thickness of the top soils above the anchor at a depth of 190 m. The inner tube is fixed to the bottom of the well and has no direct contact with the surrounding soil. Accordingly, the inner tube is not affected by soil deformations which occur shallower than 190 m depth. Thus, we can monitor the deformations of the shallow soils by measuring the differential movements of the ground surface with respect to a reference point on the inner tube.

In this study, we made use of the facilities to install a GPS station that is directly attached to the inner

tube of the well. This GPS station is expected to be less affected by the anomalous seasonal deformations because the inner tube is anchored to the bottom of the well at 190 m depth, and because groundwater for irrigation is known to be extracted mostly from aquifers shallower than 190 m (Tobita et al., 2004). Thus we expect this station to serve in better conditions as a reference station.

In this preliminary report, we first describe the structure of the GPS station. Then we compare the time series of GPS-derived vertical displacements between the station and a nearby GPS station with independent measurements such as subsidence-meter and leveling, and discuss limiting factors in the quality of this station under the present design, which should be overcome before it is fully utilized as a reliable reference station.

2. Outline of the GPS station

The GPS station, hereafter referred to as “06S061”, was installed in the subsidence monitoring observatory in the premises of GSI, which houses the subsidence-meter (Fig. 1). The GPS station is situated within a few hundred meters of other GPS stations including *TSKB*, registered with the International GNSS Service (IGS), and *TSUKUBA32*.

Fig. 2 shows the structure of the GPS station. We cut a hole on the roof of the subsidence observatory, and attached the extension pipe to the inner tube so that the GPS antenna mounted on its top sits above the roof to ensure visibility of the sky. The hole and the antenna are capped with the radome attached to the roof itself. The extension pipe is made of carbon fiber reinforced plastic (CFRP) for its strength as well as for its low thermal expansion coefficient (less than $1 \times 10^{-6} / C^{\circ}$). The set of a Trimble choke-ring antenna (*TRM29690*) and a Trimble 5700 receiver are used as recording equipment. The station became operational in April, 2007.

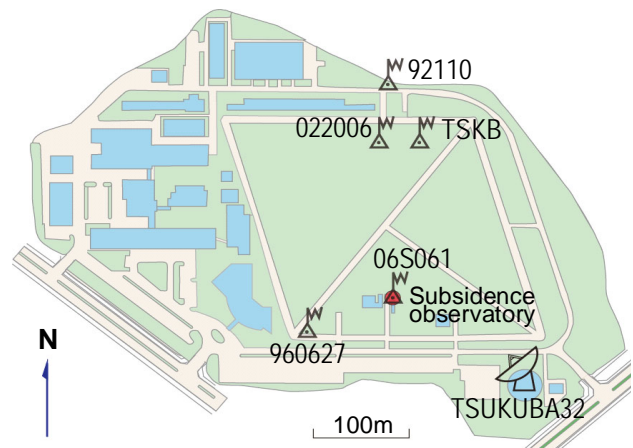


Fig. 1 Location of the deeply-anchored GPS station in the subsidence monitoring observatory in Tsukuba. Locations of other GPS stations and the VLBI station are also shown.

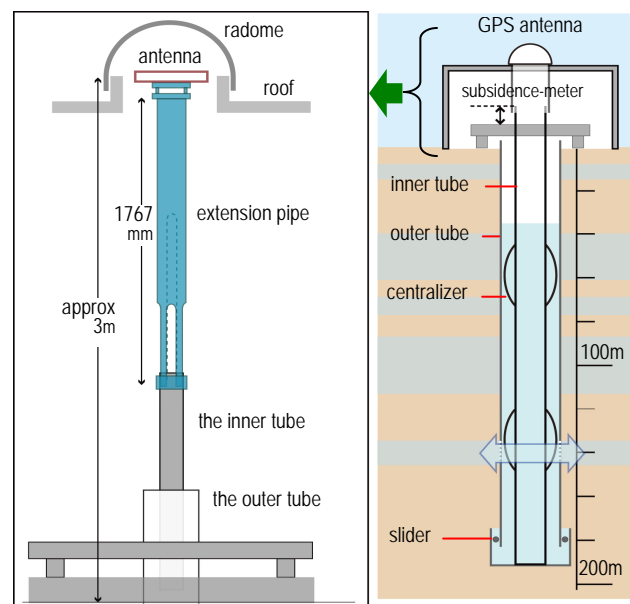


Fig. 2 A schematic figure of the structure of the GPS station 06S061.

3. Comparison of the GPS-derived vertical displacements with independent measurements

We compare GPS-derived vertical displacements with independent measurements to evaluate the quality of the GPS station 06S061. For this purpose, we first calculated the coordinate time series of surrounding GPS stations w.r.t. 06S061. We used GAMIT 10.34 (King and Bock, 2008) to analyze the data from five GPS stations

in Fig. 1 in the network-mode. We calculated two sets of solutions with different analysis strategies; 1) short-distance strategy: where we analyze GPS carrier-phases on L1 and L2 frequencies independently to estimate baseline components only, and 2) long-distance strategy: where we analyze ionosphere-free combinations of GPS carrier-phases on L1 and L2 frequencies to estimate tropospheric delays as well as baseline components.

We made two types of independent measurements for comparison. One is the subsidence-meter which records continuously the differential vertical displacements of the ground surface w.r.t. the reference point on the inner tube. The other is leveling which observes the differential heights of the surrounding GPS stations w.r.t. the reference point on the inner tube. The observations have been repeated approximately monthly.

It is empirically known that the displacements by the subsidence-meter may contain artificial coseismic offsets associated with earthquakes. Therefore, we first corrected for the coseismic offsets in the subsidence-meter measurements so that the artificial misalignment between the displacements measured by the subsidence-meter and by the leveling observations are minimized.

In Fig. 3, we compared the vertical displacements between *06S061* and its closest GPS station *960627* in the short-distance and long-distance strategies with those measured by the subsidence-meter and leveling. We see that the GPS-derived vertical displacements in the short-distance strategy agree well with those measured by both the subsidence-meter and leveling, while those in the long-distance strategy systematically disagree. In Table 1, we summarize statistics of the differences in vertical displacements between the GPS solutions and the subsidence-meter and leveling observations. It is clearly shown that the GPS-derived vertical displacements in the long-distance strategy, as compared to those in the short-distance strategy, deviate much from those by the subsidence-meter and leveling observations in terms of both the RMS and maximum difference.

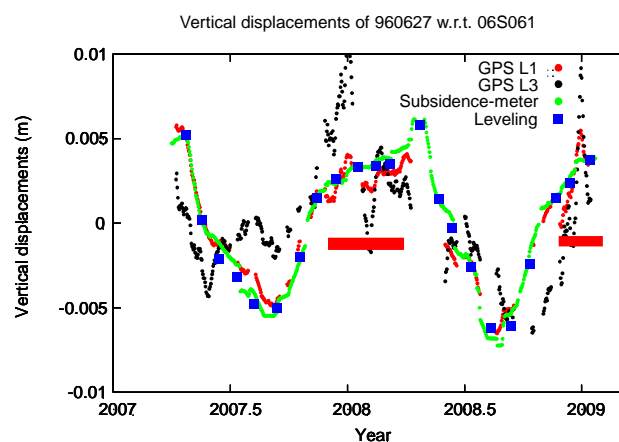


Fig. 3 GPS-derived vertical displacements of *960627* w.r.t. *06S061* and those from the subsidence-meter and leveling. All time series are de-trended, and both of the GPS-derived time series are averaged with a moving window of 10 days. Thick red bars indicate the periods when the large fluctuations of the GPS-derived vertical displacements are observed, which occur typically in winter. Red solid circles, marked ‘GPS L1’, show the displacements in the short-distance strategy and black solid circles, marked ‘GPS L3’, are those in the long-distance strategy.

Table 1 Statistics of the differences in vertical displacements between the GPS solutions at *960627* w.r.t. *06S061* and the subsidence-meter and leveling observations. The RMS and maximum difference are summarized. Note that the GPS-derived vertical displacements are averaged with the same 10-day moving window as that in Fig. 3.

Solution type	Short-distance strategy		Long-distance strategy	
	RMS diff. (m)	Max diff. (m)	RMS diff. (m)	Max diff. (m)
Leveling	0.0007	0.0014	0.0023	0.0044
Subsidence-meter	0.0009	0.0024	0.0033	0.0077

One can also see that the GPS-derived vertical displacements fluctuate larger during the periods in winter as highlighted by the thick red bars in Fig. 3. The amplitudes of fluctuations are larger in the long-distance strategy than in the short-distance strategy, though fluctuations are still noticeable in the short-distance strategy as well.

4. Investigation of error sources of the GPS-derived vertical displacements

4.1 Errors of the GPS-derived vertical displacements in the long-distance strategy

In section 3, we showed that the GPS-derived vertical displacements in the long-distance strategy systematically disagree with those by the subsidence-meter and leveling observations. Here we investigate possible sources that cause such errors.

We first examined the zero-difference phase residuals of the GPS solutions in the short-distance strategy. In Fig. 4 we present the phase residual maps at two stations, *06S061* and *960627*, averaged for January, 2008 as examples. One can see that phase residuals obtained at *06S061* are significantly larger than those at *960627*.

It is likely that the direction-dependent errors in GPS carrier-phases at *06S061* as shown in Fig. 4 leak into the vertical components of the GPS solutions in the long-distance strategy since the GPS solutions in the long-distance strategy are known to be more susceptible to noises in GPS carrier-phases than those in the short-distance strategy, especially when tropospheric parameters are simultaneously estimated. Here, we tested this possibility. For this purpose, we stacked the phase residuals of GPS solutions in the short-distance strategy on a monthly basis and generated “monthly-average noise maps”. Then, we reanalyzed the GPS data in the long-distance strategy with correction for the errors in GPS carrier-phases using a corresponding monthly-average noise map.

The vertical displacements in the long-distance strategy with the correction are plotted in Fig. 5. One can see that the GPS-derived vertical displacements in the long-distance strategy after correction follow those in the

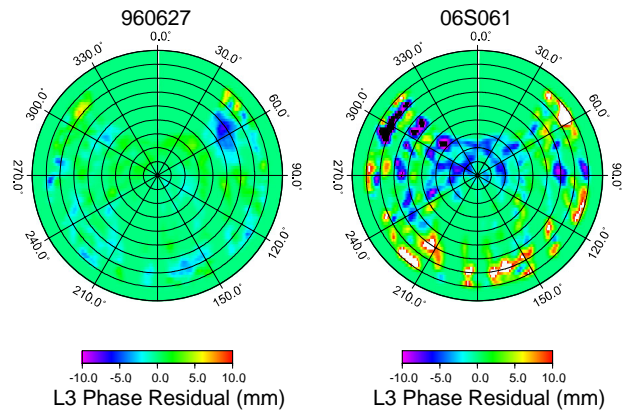


Fig. 4 Monthly-averaged phase residuals of the GPS solutions in the short-distance strategy at two stations, *06S061* and *960627* for January, 2008. The phase residuals are those for the ionosphere-free combinations. Azimuths are measured clockwise from the north.

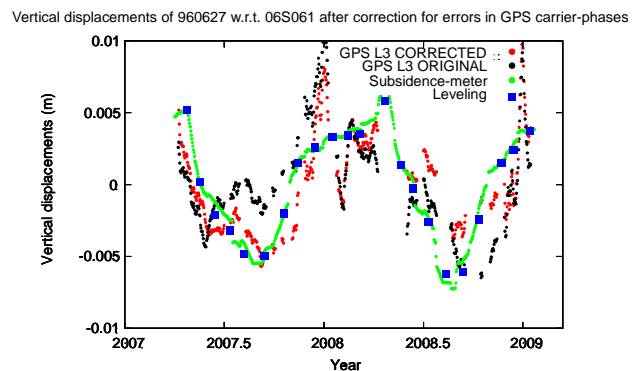


Fig. 5 GPS-derived vertical displacements of *960627* w.r.t. *06S061* in the long-distance strategy after correction for the errors in GPS carrier-phases.

short-distance strategy better. In Table 2 we summarize the statistics of the differences in vertical displacements between the GPS solutions with/without correction for the errors in GPS carrier-phases and the subsidence-meter and leveling observations. From Table 2, it is clear that the correction reduces discrepancies greatly in terms of both the RMS and maximum difference. Thus, we confirmed that the direction-dependent errors in GPS carrier-phases at *06S061* induced large errors of the GPS-derived vertical displacements in the long-distance strategy.

Then, the question arises what caused the errors

in GPS carrier-phases at 06S061? Since the antenna is set close to the roof as shown in Fig. 2, one possible cause may be the multipath due to the reflection of GPS radio-waves from the metallic roof of the housing. This will explain why the discrepancies between the vertical displacements in the long-distance solution and those from the subsidence-meter and leveling are systematic since the multipath will vary systematically according to seasonal distance changes between the antenna and the roof.

We conducted experimental measurements at 06S061 to affirm this possibility. Two countermeasures were adopted to avoid the multipath from the roof. One is to separate the antenna as far as possible from the roof surface, and the other is to lay radio-wave absorbers over the roof surface. Fig. 6 shows the layout of the experimental countermeasures. The same choke-ring antenna was mounted on top of a tripod at a height of exactly 1 m above the roof surface and radio-wave absorbers were laid around the tripod on top of the roof.

We analyzed the data obtained with these settings in the short-distance strategy to see whether phase residuals are effectively reduced or not. Fig. 7 shows the phase residuals thus obtained. The phase residuals are largely reduced compared to those in Fig. 4. This result indicates that 1) the large phase residuals of the GPS solutions in the short-distance strategy are caused by the multipath from the roof surface, and 2) the multipath effects are mitigated by placing the antenna off the roof surface and by laying radio-wave absorbers in the proximity of the antenna.

4.2 Errors of the GPS-derived vertical displacements in winter

Next, we investigated causes of large fluctuating errors in the GPS-derived vertical displacements observed only in winter. Under the suspicion of environmental deterioration of GPS signal acquisition, we watched around the environmental conditions at 06S061 when large errors were recognized in the time series of GPS solutions. There we noticed many water droplets inside the radome (Fig. 8).

Table 2 Statistics of the differences in vertical displacements between the GPS solutions in the long-distance strategy and those from independent measurements. Two types of GPS solutions with and without correction for the errors in GPS carrier-phases are considered.

Solution type	Long-distance strategy (original)		Long-distance strategy (after correction)	
	RMS diff. (m)	Max diff. (m)	RMS diff. (m)	Max diff. (m)
Leveling	0.0023	0.0044	0.0019	0.0042
Subsidence-meter	0.0033	0.0077	0.0025	0.0066

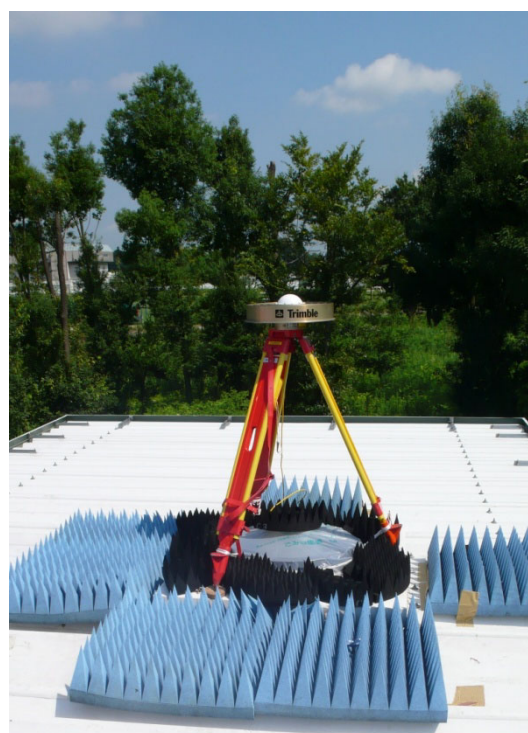


Fig. 6 The layout of the experiment at 06S061 for evaluating the effects of multipath from the roof surface. The antenna is mounted on top of the tripod at a height of 1 m above the roof surface. The radio-wave absorbers (black or blue sheets with spikes) are laid on the roof surface.

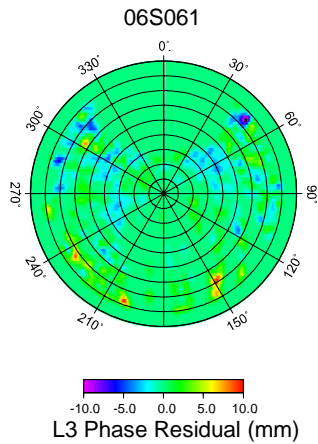


Fig. 7 Phase residuals of the GPS solutions in the short-distance strategy at *06S061* during the experiment. The phase residuals are those for the ionosphere-free combinations, the same as in Fig. 4. Note that residuals are reduced greatly compared to those in Fig. 4.



Fig. 8 The inside of the radome of *06S061* when the large errors in the vertical displacements time series are observed. Many water droplets are seen on the surface.

These droplets are presumably formed by water condensation in the air of the observatory. The observatory is lagged with two-fold walls, the outer wall of which is filled with high thermal insulation materials. The radome, on the other hand, stands in the outer air. Therefore, the large difference in temperature between the outside and the inside of the observatory results in water condensation on the radome inside the observatory.

For a control experiment, we wiped the droplets

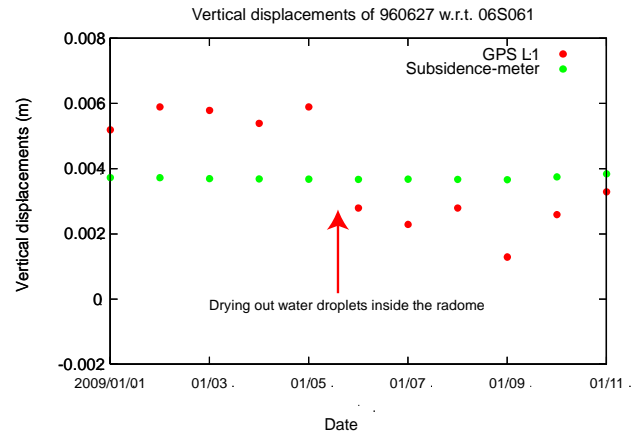


Fig. 9 Vertical displacements of *960627* w.r.t. *06S061* before and after wiping out water droplets inside the radome of *06S061*. The red arrow denotes the date of the wipe-out.

from the radome and continued GPS observation. We compared the GPS-derived vertical displacements in the short-distance strategy before and after wiping. As seen in Fig. 9, we found that the large offsets of the GPS-derived vertical displacements against those from the subsidence-meter are largely mitigated after wiping. The shift in the GPS-derived vertical displacements after wiping amounts to as large as 3 mm.

It is known that water droplets on a radome affect GPS-signal propagation due to their dielectric property. For example, Wübbena et al. (2008) investigated such effects on the estimated coordinate time series using an artificially sprinkled radome with a choke-ring antenna and found that water droplets on a radome surface caused errors in the GPS-derived coordinate time series as large as 4 mm. Thus, it is likely that water droplets formed inside the radome are responsible for the large errors in the GPS-derived vertical displacements at *06S061* in winter.

5. Concluding remarks

We evaluated the quality of the deeply-anchored GPS station installed in the premises of GSI in Tsukuba by comparing the GPS-derived vertical displacements with those from the subsidence-meter and the leveling observations. We find that the station is affected by the multipath from the metallic roof of the housing. We also reveal that water droplets formed inside the radome due

to water condensation in the room's air in winter caused large errors in the GPS-derived vertical displacements time series.

We are now upgrading the structure of GPS station *06S061*: the GPS antenna will be pulled up 1 m higher, radio-wave absorbers are laid over the roof, and the radome and GPS antenna are isolated from the room's air. These countermeasures should reduce the multipath from the rooftop and water condensation inside the radome. The quality of the upgraded station will be reported elsewhere.

Acknowledgements

We are indebted to the Environmental Geography Division, Geographic Department of GSI for providing the subsidence-meter data. We thank Ms. F. Hayashi for her help in manuscript preparation. The study has been carried out as a project entitled 'research on precise maintenance of geodetic datum' under the auspices of Special Research Budget of the Geographical Survey Institute.

References

- Z. Altamimi, X. Collilieux, J. Legrand, B. Garayt, and C. Boucher (2007): ITRF2005: A new release of the International Terrestrial Reference Frame based on time series of station positions and Earth Orientation Parameters, *Journal of Geophysical Research*, 112, B09401, doi:10.1029/2007JB004949.
- Y. Hatanaka, A. Yamagiwa, T. Yutsudo, and B. Miyahara (2005): Evaluation of precision of routine solutions of GEONET, *Journal of the Geographical Survey Institute*, 108, 49-56 (in Japanese with English abstract).
- R. W. King and Y. Bock (2008): Documentation for the GAMIT GPS analysis software release 10.34, Massachusetts Institute of Technology, Cambridge.
- H. Munekane, M. Tobita, and K. Takashima (2004): Groundwater-induced vertical movements observed in Tsukuba, Japan, *Geophysical Research Letters*, 31, L12608, doi:10.1029/2004GL02158.
- M. Tobita, H. Munekane, M. Kaidzu, S. Matsuzaka, Y. Kuroishi, Y. Masaki, and M. Kato (2004): Seasonal variation of groundwater level and ground level around Tsukuba, *Journal of the Geodetic Society of Japan*, 50, 27-37 (in Japanese with English abstract).
- G. Wübbena, M. Schmitz, and M. Propp (2008): Sensibility of Dorne Margolin chokering antennas to rainfall-analysis of sprinkled antenna site on a short-baseline, paper presented at IGS analysis workshop, June 2-6, Miami Beach, Florida.